ION EXCHANGE AND ADSORPTION
ISSN: 1001-5493
Vol. 23, Issue-02, 2023
pp.44-60

SYNTHESIS, SPECTRAL, DFT, MOLECULAR DOCKING AND ADMET PROPERTIES OF DIBENZYLOXY CHALCONES

Dr. S. Prabha
Associate Prof, Dept. of Chemistry, Govt. Arts College, Chidambaram, Tamilnadu, Inia-608102.

Abstract

Present article has included the preparation of unsubstitted, *p*-methoxy and *p*-nitro substituted dibenzxyloxy chalcones (**1-3**) with the help of ultrasonic energy. The formation of chalcones was confirmed by their spectral data. The DFT analyses of chalcones (**1-3**) were done and the dcalculated values are compared with literature values. Further, molecular docking with Sars-Cov-2 (pdb id : 6w63) for all chalcones (**1-3**) were performed and the results are compared. The pre-ADMET properties, drug-likeness and toxicity parameters are observed and discussed.

Key words *: Chalcones; UV, IR and NMR spectra; DFT analysis; Molecular docking; ADMET property*

1. Introduction

In 1899, the scientists namely Kostanecki and Tambor have given the compounds having α,β-unsaturated ketones as chalcones. Such compounds may be natural or synthetic which belong to the bicyclic Flavonoid family [1].They are both intermediates and end products in Flavonide biosynthesis [2]. Chalcones has been targeted by several researchers in recent years due to their wide biological potential [3], as well as their ability to serve as important intermediates for the synthesis of a large number of heterocyclic systems[4]. The structural skeleton of chalcones especially 1,3 – diarylprop –2-en- 1 – ones are constituted by two aromatic rings linked through the open chain three-carbon unit α, β – unsaturated carbonyl system[4] (**Scheme-1**) .

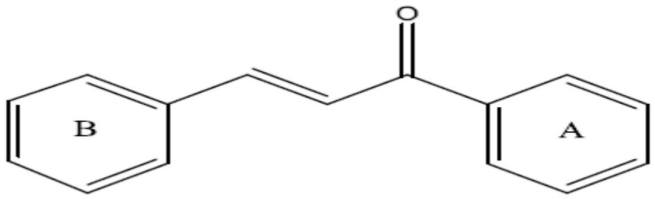

Scheme-1: Chemical structure of chalcone

The presence of chromophore (-CO-CH=CH-) and auxochromes give these compounds the colour, hence their ecological role in relation to plant colour. These bright yellow compounds are found in many plant organs[5,6]. Chalcones or 1,3-diarylpropenones are used as a starting material to synthesize many of the heterocyclic ring systems like pyrazolines, isoxazoles, pyrimidines and cyanopyridines. this compound forms a central core for a variety of important biological compounds[2], which are used as an antioxidant[7], anticancer[8], antibacterial[9], antifungal[10], anti-inflammatory[11], and Antiviral[12] depending on the substitution made on them[13]. The chemistry of chalcones has developed intensive scientific studies throughout the world. Chalcones exist as either *E* or *Z* isomers, the *E*- isomer being in most cases the thermodynamically most stable form and consequently, the majority of the chalcones is isolated

as the *E* -isomer [14]. The interesting electronic and nonlinear optical properties of chalcones derivatives act as a trigger towards exploring different and new applications. For assessing the spectral as well as structural properties of organic molecules, theoretical calculations like Density Functional Theory method (DFT) have developed as a powerful technique. Most of the DFT studies have been published describing a broad range of chalcones properties [15, 16]. The characterization of synthesized novel chalcones by substitution groups in their derivative structures was also achieved using DFT [17, 18]. Molecular docking is an effective strategy to gain insight into ligand-receptor interactions in the drug design industry. The vital role of molecular docking in the development of drug design is due to its ability to predict the best binding mode between drugs and the target protein. Molecular docking methods were used widely to analyze the biological and antibacterial activities of chalcones [19-21].

In pandemic period, SARS-CoV-2 is a virus from the Coronavirus group that spreads very quickly throughout the world and causes COVID-19 disease in millions of people worldwide. SARS-CoV-2 infects host cells by involving several proteins from the virus and proteins from the host. Main protease SARS-CoV-2 or chymotrypsin-like protease (3CLpro) is a protein that plays a role in the viral replication process and is very important for the life cycle of life SARS-CoV-2 [22. Therefore, 3CLpro main protease is one of the potential targets in treating COVID-19. Until now, a drug has not been explicitly found used to treat COVID-19. Treatment therapy for COVID-19 patients is administering drugs that have been circulating. These drugs are antiviral drugs such as oseltamivir, ritonavir, lopinavir, and remdesivier. The other treatment is using antimalarial drugs such as chloroquine phosphate. As it is Covid time as well as a pandemic time, SARS-CoV-2 spike protease is chosen by several researchers in order to knowing their molecular docking study. Chalcone-derived compounds can be antivirals against the Coronavirus class through the primary protease inhibitory mechanism. Park et al., [23] showed that chalcone-derived compounds isolated from the *Angelica keiskei* plant could inhibit the protease enzyme (3CLpro) SARS-CoV activity. Brousso chalcone A and B isolated from the roots of *Broussonetia papyrifera* were shown to inhibit 3CLpro SARS-CoV and 3CLpro MERS-CoV [24]k et al., 2017). Therefore, chalcone compounds and their derivatives may also have inhibitory activity against 3CLpro SARS-CoV-2. Several in silico studies through molecular docking of chalcone-derived compounds have been carried out, such as the indole-chalcone-derived compound that was docked against the main protease SARS-CoV-2 (GDP: 6YB7) [25] and (E)-1-(2,4-dichlorophenyl)-3-[4-(morpholin-4-yl)phenyl]prop-2-en-1-one with *main protease* SARS-CoV-2 (GDP: 7BQY) [26].

Hence, the continuation of synthesized chalcones (**1-3**), we have planned to study docking study using SARS-CoV-2 spike protease. This paper reports the synthesis, spectral characterization, DFT calculations of chalcones (**1-3**) and their molecular docking against spike protease.

2. Experimental

2.1. Materials and methods

All chemicals were purchased commercially and used without prior purification. Melting points were determined in open capillary tube and were uncorrected. Elemental analyzes were carried out on Variomicro V2.2.0 CHN analyzer. FT-IR spectrum of title compounds were recorded on a Shimadzu FTIR spectrophotometer in the range 400–4000 cm^{-}

[1] using the KBr pellets. The proton and carbon NMR spectra were recorded on a BRUKER AVANCE III 500MHz NMR spectrometer using $CDC1_3$ as solvent. Chemical shifts were reported in ppm. Tetramethylsilane (TMS) was used as internal reference for all NMR spectra, with chemical shifts reported in units (parts per million) relative to the standard. ^{1}H NMR signal patterns are indicated as singlet (*s*), doublet (*d*), doublet of doublet (*dd*), triplet (*t*), quartet (*q*) and multiplet (*m*). The FT-IR are recorded at Department of Chemistry, Annamalai University and NMR spectra are recorded at SAIF, IIT, Chennai.

2.2 Synthesis of compounds

2.2.1 Synthesis of *(E)-1-(3,5-bis(benzyloxy)phenyl)-3-phenylprop-2-en-1-one* (1)

In a 100mL conical flask, equimolar quantity of 1-(3,5-bis(benzyloxy)phenyl)ethanone (2.5 mmol) and benzaldehyde (2.5 mmol) were taken with absolute ethanol (5 mL) and 40 % sodium hydroxide (20 mmol diluted to 2 mL). The mixture was then immersed to ultrasonic bath at room temperature [27] for 2 min. The completion of the reaction was monitored by thin-layer chromatography (eluent 20:80: ethyl acetate: hexane). After completion, the resulting mixture was acidified by using dilute HCl and the precipitate was filtered. The product formed was recrystallized from hot ethanol. The general scheme for preparation of compounds **1, 2** and **3** are given in **Scheme-2**. The synthesized pure products were characterized by UV, FT-IR, ^{1}HNMR, ^{13}C NMR and Mass analytical methods.

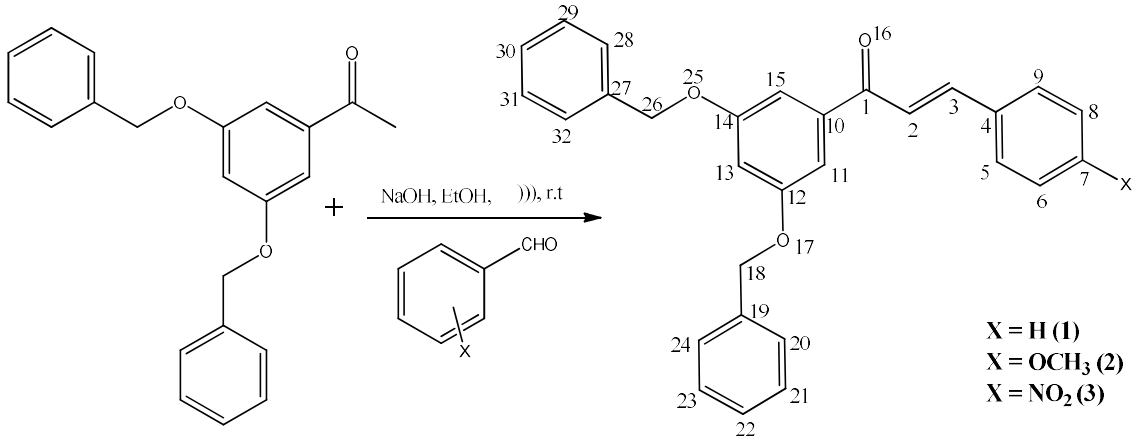

Scheme-2 : Synthetic scheme of chalcones (**1, 2** and **3**)

2.3. Computational study

Geometry optimizations were carried out according to density functional theory using B3LYP/6-31G(d,p) basis set in the Gaussian-09 package[28]. The polarizabilities and hyperpolarizabilities have been derived from the DFT optimized structure by using finite discipline technique using the B3LYP/6-31 G basis set available in Gaussian-09.

3. Results and Discussion

3.1 Spectral analysis

The physical and spectral measurements of the synthesised compounds are given below.

3.1.1 Spectral analysis of *(E)-1-(3,5-bis(benzyloxy)phenyl)-3-phenylprop-2-en-1-one* (1)

Yield 83%; mp 121-122 ˚C; m/z 420; UV (CH_3OH, λ_{max}^{nm}) 318.00, IR (KBr, νcm^{-1}) 3061-2886 (Ar. CH str), 1660.71 (C=O), 1585.49 (Ar C=C str), 1215.15 (CH_{ip}), 918.12 (CH_{op}), 1024.20 (Ali. CH=CH_{op}), 565.14 (Ali. C=C_{op}). ^{1}H NMR (500 MHz, $CDCl_3$, δ/ppm) d 6.864(1H, *d*, J = 15 Hz), 7.251 (1H, *d*, J = 15 Hz), 5.139 (4H), 7.285–7.662 (16H,overlapping m, ArH); ^{13}C-NMR (125 MHz, $CDCl_3$, δ/ppm) 122.066 (C_α), 144.966 (C_β), 189.989(CO), 29.713 (O-CH_2-), 106.660-160.084 (Ar. Carbons).

3.1.1 Spectral analysis of *(E)-1-(3,5-bis(benzyloxy)phenyl)-3-(4-methoxyphenyl)prop-2-en-1-one* (2)

Yield 76%; mp 126-127 ˚C; m/z 450; UV (CH_3OH, λ_{max}^{nm}) 327.00, IR (KBr, νcm^{-1}) 3072-2848 (Ar. CH str), 1664.57 (C=O), 1587.42 (Ar C=C str), 1253.73 (CH_{ip}), 939.33 (CH_{op}), 1043.49 (Ali. CH=CH_{op}), 526.57 (Ali. C=C_{op}). ^{1}H NMR (500 MHz, $CDCl_3$, δ/ppm) d 7.252(1H, *d*, J = 15 Hz), 7.791, (1H, *d*, J = 15 Hz), 5.114 (4H), 7.334–8.470 (15H,overlapping m, ArH); ^{13}C-NMR (125 MHz, $CDCl_3$, δ/ppm) 125.645 (C_α), 142.847 (C_β), 189.187(CO), 30.927 (O-CH_2-), 29.705 (O-CH_3) 107.483-160.176 (Ar. Carbons).

3.1.1 Spectral analysis of *(E)-1-(3,5-bis(benzyloxy)phenyl)-3-(4-nitrophenyl)prop-2-en-1-one* (3)

Yield 79%; mp 131-132 ˚C; m/z 465; UV (CH_3OH, λ_{max}^{nm}) 342.00, IR (KBr, νcm^{-1}) 3082-2880 (Ar. CH str), 1664.57 (C=O), 1593.20 (Ar C=C str), 1168.86 (CH_{ip}), 979.84 (CH_{op}), 1041.56 (Ali. CH=CH_{op}), 518.85 (Ali. C=C_{op}). ^{1}H NMR (500 MHz, $CDCl_3$, δ/ppm) d 7.528(1H, *d*, J = 15 Hz), 7.792 (1H, *d*, J = 15 Hz), 5.118 (4H), 6.861-8.474 (15H,overlapping m, ArH); ^{13}C-NMR (125 MHz, $CDCl_3$, δ/ppm) 122.434 (C_α), 141.746 (C_β), 189.181(CO), 29.698 (-O-CH_2-), 107.017-160.181 (Ar. Carbons).

3.2 DFT analysis

In the present study, the author has synthesized three number of diaryl prop-2-en-1-ones and characterized them with the help of spectral techniques. The Density Functional Theory analysis of these compounds (**1-3**) were performed using the Guassian 09 programme with 6-31G(d,p) basis set and the compounds are visualized at Gaussview 5.0.8 software. The obtained results are discussed below.

Geometry and its parameters

All the synthesized chalcones or diaryl prop-2-en-1-ones (**1-3**) are optimized and their optimized structures are given in **Fig. 1**. Some of the selected bond lengths calculated for these systems (**1-3**) are displayed in **Table-1** along with bond angles and dihedral angles.

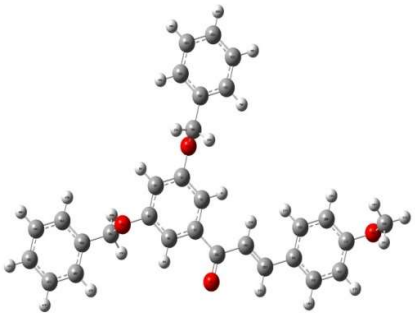

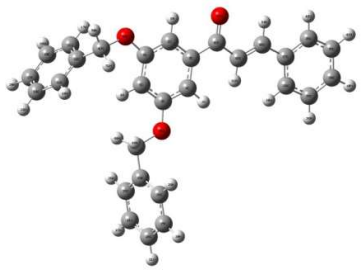

(1) **(2)**

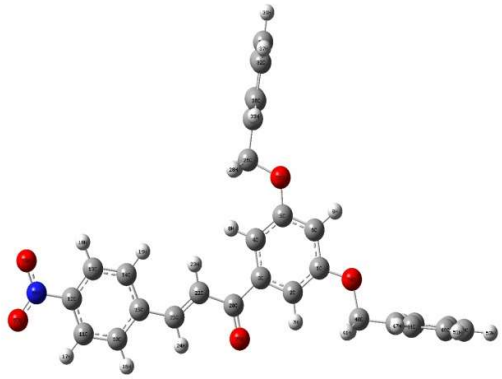

(3)

Figure-1 : Optimized structure of chalcones **1-3**

The bond length between the carbonyl group C1-O2 is calculated as ~1.26A° for all the t compounds (**1-3**). The vinyl bond length C2-C3 and C2/3-H2/3 in α and β positions are calculated as 1.35 and 1.08 respectively. These calculated lengths are agreed with literature values [29]. The bond angles between C10-C1-O16 are calculated as 119 by DFT method. The other calculated angles O16-C1-C2 and C1-C2-C3 ~120 are agreed with literature values. The angle between C7-O33-C-34 is calculated nearly 117 for compound **2** and it is slightly distorted from the phenyl ring. The dihedral angles C1-C2-C3-C4 and C10-C1-C2-C3 of compounds **1-3** shows nearly 179 and it clearly indicates that all the synthesized compounds (**1-3**) have exhibited in *trans* form and cal. values are agreed good with previous values.

Table -1: Selected geometrical Parameters of the compounds **1-3**

Bond length (A°)	**1**	**2**	**3**	**Bond angle** (°)	**1**	**2**	**3**
C4-C5	1.4	1.4	1.4	C5-C6-C7	120	120	120
C1-O16	1.26	1.26	1.26	C10-C1-C2	119	119	120
C1-C2	1.47	1.47	1.48	O16-C1-C2	120	120	120
C2-C3	1.35	1.35	1.35	C1-C2-C3	120	120	120
C2-H2	1.08	1.08	1.08	C2-C3-C4	128	120	127
C3-H3	1.08	1.08	1.08	C12-O17-C18	119	119	119
C10-C1	1.49	1.49	1.49	O17-C18-C19	107	107	107
C12-O17	1.39	1.39	1.38	C11-C12-O17	120	120	120
O17-C18	1.47	1.46	1.47	C7-O33-C34		117	
C18-C19	1.5	1.5	1.5	C7-N33-O34/35			118
C18-H18	1.09	1.09	1.09				
C7-O33 / C7-N33		1.38	1.46				
O33-C34/N33-34		1.45	1.26				
Dihedral angle (°)	**1**	**2**	**3**				
C10-C1-C2-C3	128	129	176				
C1-C2-C3-C4	179	179	179				
O16-C2-C3-H3	177	180	174				
H2-C2-C3-H3	180	180	179				
C14-H25-C26-C27	180	178	179				

C12-O17-C18-C19	180	180	179
O17-C18-C19-C20	96	93	96

Vibrational analysis

The experimental IR spectra of the compounds (**1-3**) were recorded and compared with the theoretical frequencies calculated by DFT method and the values are given in **Table-2** . The carbonyl group has characteristic band at 1660-1664 cm^{-1} for compounds **1- 3** in experimental. The frequencies are calculated at 1631-1646cm^{-1} by B3LYP method [30]. The aromatic C-H stretching are observed nearly 3082-3062cm^{-1} by experimentally and calculated in the region of 3150-3077cm^{-1} [31]. The aromatic –C=C- stretching is observed at 1585, 1587, 1593cm^{-1} and calculated at 1646, 1631 and 1639 respectively for compounds **1-3**. The –CH inplane bending deformaions for phenyl ring are observed experimentally nearly 1215-1168 cm^{-1} [32] and the values are calculated nearly 1213-1226cm^{-1}. For compound **2**, the C-O-C stretching for methoxy group is observed at 1253 cm^{-1} and calculated at 1238 cm^{-1} [33]. The NO_2 stretching for **3** is calculated 1285 and 1485cm^{-1} and observed at 1359cm^{-1}.

Table-2 : IR frequencies of Experimental and DFT (scaled) method of compounds **1-3**

DFT scaled (cm^{-1}) 1	**Exp. IR (cm^{-1})** 1	**DFT scaled (cm^{-1})** 2	**Exp. IR (cm^{-1})** 2	**DFT scaled (cm^{-1})** 3	**Exp. IR (cm^{-1})** 3	**Assignment**
3135		3134		3136		sym str CH
3131		3131		3131		sym str CH
3101		3099		3100		sym str CH
3099		3094		3097		sym str CH
3079	3061	3087	3072	3077	3082	sym str CH
		3061	2924			asy str CH_3
		2989				asy str CH_3
3029	3031	2965	2846	2972	2880	asy str -CH_2-
2961	2924	2952		2959		asy str -CH_2-
1646	1660	1631	1664	1639	1664	sym str C=O
1609	1585	1603	1587	1603	1593	sym str C=C
1606		1591		1592		sym str C=C
1602		1583		1590		sym str C=C
1580		1580		1575		sym str C=C
1574		1556		1573		sym str C=C
1550		1534		1542		sym str C=O, C=C
1500	1490	1507	1440	1507	1442	CH_2-def
1496		1498		1499		CH_2-def
1495		1495		1491		βCH (phenyl)
1492		1488		1462		βCH (phenyl)

1469		1473		1455		βCH (C=C)
		1238	1253			sym str C-O (-C-OCH_3)
				1427	1359	asy NO_2
				1392		asy NO_2
				1235		sym NO_2
1165	1165	1167	1165	1178	1168	ϒCH (phenyl)
1131		1139		1125		ϒCH (phenyl)
1345		1354		1345		ϒCH (phenyl)
1339		1336		1335		ϒCH (phenyl)
1021	1024	1024	1043	1082	1041	ϒCH (C=C)
1007		1008		1073	912	ϒCH (C=C)
1007	918	1014	939	1014		ϒCH $_{op}$
574	565	574	526	576	518	ϒC=C $_{op}$

Non-Linear Optical property

In the field of telecommunications, optical interconnections and optical memory for emerging in the area of signal processing, the nonlinear optical organic materials has significant role. These organic materials exhibit high polarizability and delocalized π conjugated electronic structure. These structures enable passage of electron contributor and acceptor groups from single side of molecule to the other side and provide widespread range of usages in NLO, engineering and synthesizing the chemicals. Due to the charge distribution or transfer from one side to another side makes the molecule as polarized. In the present study, the calculated dipole moments (**μ**), polarizabilities (α_{tot}) and first order hyperpolarizabilities (β_{tot}) are given in **Table-3**.

Table-3 : Dipole moments and Polarizabilities of compounds **1-3**

Parameters	**1**	**2**	**3**
Dipole moments (Dynes)	4.495	2.616	4.304
Polarizability			
α_{xx}	-146.64	-143.74	-255
α_{xy}	8.32	14.89	12.21
α_{yy}	-190.42	-176.93	186.01
α_{xz}	2.71	-0.98	3.92
α_{yz}	-2.21	-2.83	0.38
α_{zz}	-187.9	-196.14	-193.17
<α> (a.u)	174.99	172.27	87.39
α_{tot} x 10^{-24}(esu)	25.93	25.53	12.95
Hyperpolarizabilities			
β_{xxx}	148.08	-408.67	945.13
β_{xxy}	37.38	-254.7	-51.01

β_{xyy}	-18.1	-40.56	-15.98
β_{yyy}	115.28	93.71	146.66
β_{xxz}	47.71	-18.1	-32.61
β_{xyz}	-8.28	-20.48	-8.82
β_{yyz}	19.04	21.82	-0.73
β_{xzz}	-54.4	8.64	17.75
β_{yzz}	-19.36	30.19	13.33
β_{zzz}	0.3	-40.56	3.31
β_{tot} (a.u)	167.26	89.63	953.63
β_{tot} x 10^{-30}(esu)	1.445	3.983	8.238

Standard: Urea has a β value of 0.65 x10^{-30} esu [34].

The dipole moments clearly indicate that all the compounds (**1-3**) are mainly attributed to an overall imbalance in charge. All the compounds have significant NLO property when compared with standard urea [34] and compound **3** is higher NLO activity [35] than others. The observed β_o values are several times greater than standard urea which is a typical NLO material.

Frontier Molecular Orbital energies

Molecular orbital energies are an effective tool that plays an important role in both electrical and optical properties of quantum chemistry. The two significant orbitals called HOMO and LUMO define the conjugated molecules. These are referred to as FMOs and are found at the outermost boundaries of electron molecules. The HOMO-LUMO energy was used to find out the energetic activity of the molecule using the B3LYP/6-31G(d,p) package. For compounds **1** and **2**, the HOMO is located over phenyl ring of ketone moiety and it is widespread throughout the chalcone moiety for **2**. LUMO is distributed over α,β-unsaturated ketone and phenyl ring of aldehyde taken. The diagram and energies of HOMO's and LUMO's are given in **Fig. 2** and **Table-4** with the energy gap level.

Table-4 : FMO energies of compounds **1-3**

Parameters	Calculated values		
	1	**2**	**3**
E_{Homo}(a u)	-6.436	-6.435	-6.234
E_{Lumo}(a.u)	-2.534	-2.272	-3.306
Energy gap(a.u)	3.902	4.163	2.928
Ionization energy(I)	6.436	6.435	6.234
Electron affinity(A)	2.534	2.272	3.306
Global hardness(η)	1.951	2.081	1.464
Chemical potential(μ)	-4.485	-4.353	-4.770
Electrophilicity index(ω)	5.154	4.552	7.772

Chemical softness(s)	0.513	0.4805	0.68315

The energy gap between HOMO and LUMO is an important factor for studying their rigidity and reactivity. The compound **3** has lowest energy gap and it is highly reactive than others. From the orbital energies, other parameters like Ionisation energy, hardness, electrophilicity index, chemical potentials and softness [36] are calculated and displayed in same **Table-4**. The hardness of the compound **2** is higher and is chemically less reactive than others. This is attributed to the presence of electron donating methoxy group in molecule **2**. The electrophilicity index of molecule **2** is higher and is better bioactivity than others.

HOMO **LUMO**

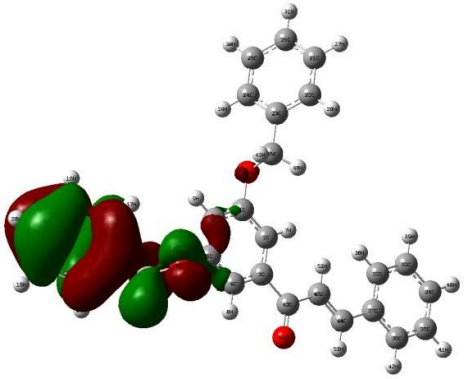

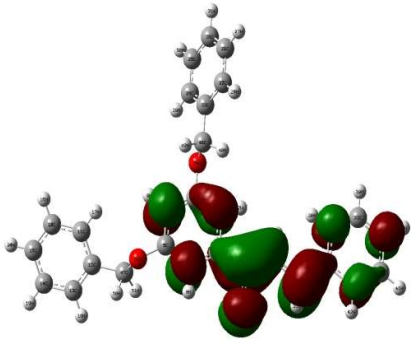

1 **1**

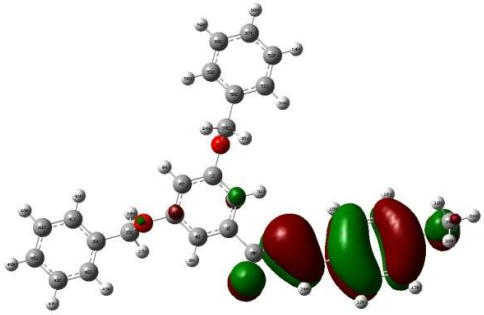

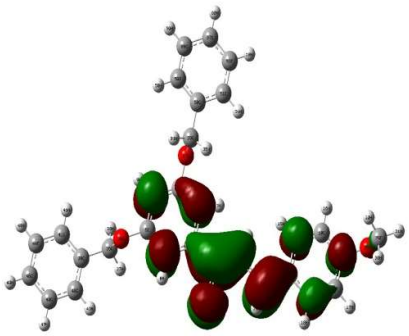

2 **2**

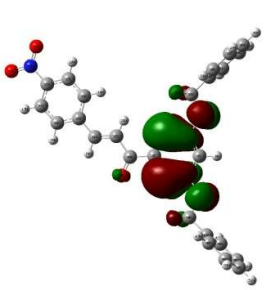

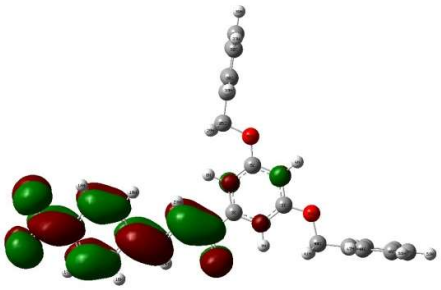

3 **3**

Figure-2 : HOMO and LUMO orbitals of compounds **1-3**

3.3 Molecular docking study

Now-a-days, the drug design for the molecular docking study plays a vital role. For the purpose of docking, many more number of docking programs is available. Generally, these programs examine the interactions and movements during the binding of ligand with protein. For the study of binding interactions, we need the three dimensional structure of ligands and proteins. In the present study, the selected protein has been downloaded as 3D structure [37] from RCSB (Protein Data Bank) (Berman et. al., 2003) according to the determined activities and the ligands are prepared and converted to pdb file. AutoDock Vina program [38] (Trott & Olson, 2010) has been used for docking study of present investigation.

` In the downloaded pdb structure of the protein, the water molecules and ligand are removed then polar hydrogen atoms were added. The optimized geometries of molecules (**1-3**) were used for PDB format as ligand. In this step, all preparations for both ligands and targets were made by with Discover Studio Visualizer 17.0 software.

Table-5 : Docking parameters of compounds **1-3** with Sars-Cov-19 protease

Compounds	1	2	3
binding energy	-8.7	-8.6	-8.7
Hydrogen Bond	2	2	3
Electrostatic interaction	1	-	-
Other interactions (Hydrophobic / pi-alkyl / pi-anion/ pi-cation)	5	6	5
Amino acid residue involved interaction	HIS163, GLU166, HIS164, THR25, CYS145, HIS41, CYS44 and MET49	GLY143, THR190, MET49, CYC145, MET165, HIS41	HIS41, THR190, GLN192, MET49 and MET165
Hydrogen Bond Distance (A°)	2.48, 2.98, 3.57	2.743. 2.744	2.74, 2.58, 2.34

The docking studies as described in literature [39-41], with the help of AutoDock Vina program, the molecular docking result outputs computed for 9 different conformational poses of the each ligand compounds (**1-3**) docked into the target receptor macromolecules (**6w63**) are listed in **Tables 5**. For molecular docking analysis, the starting ground state molecular conformational forms of the ligand compounds (**1-3**) were obtained by using DFT-B3LYP/6-311++G(d,p) computational level of theoretical model. The comments on the interaction results were performed for the best conformational poses with the lowest interacting energies obtained

of the ligand compounds docked into the target macromolecules 6w63. Additionally, in these tables inhibition constants and the number of hydrogen bonding were given in the bottom lines.

According to the affinity binding energies, the best bindings were determined for compound **1** and compound **3** with same -8.7 kcal/mol energy, and two hydrogen bonding for compound **1** and three hydrogen bonding for **3** as shown in **Table 5.** The results implied that the carbonyl group oxygen strongly binded with HIS 163 and GLU 166 residues for compound **1**. The compound **2** has binding energy of -8.6 kcal/mol with protein residue including two hydrogen bonding interactions. The other interactions like pi-alkyl, pi-sulphur, pi-anion, pi-cation, etc., interactions are seen in all compounds (**1-3**). The compound **3** has significantly strong affinity than **1** with the low hydrogen bonding distance. All the active groups are strongly involved in hydrogen bonding interactions with protease chosen. The pi-electrons of the phenyl groups, nitro group, oxygen atom of carbonyl group, methylene oxygen atoms and methoxy oxygen atom are involved in interactions with protease. On comparing these three chacolnes (**1-3**), the compound **3** has potentially active than other two chalcones (**1-2**). The interactions obtained from molecular docking results as 3D (a) and 2D (b) forms are shown in **Fig. 3**.

Although we cannot say the statement precisely because we do not have experimental data, these results concluded that the compounds are potent inhibitor.

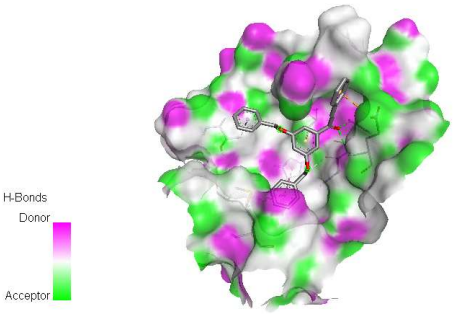

3D docking pose of **1**

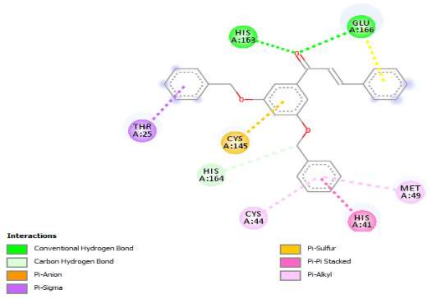

2D docking pose of **1**

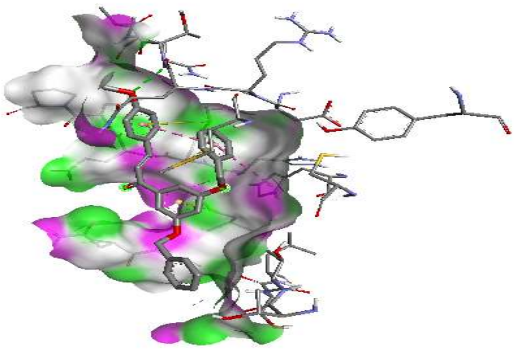

3D docking pose of **2**

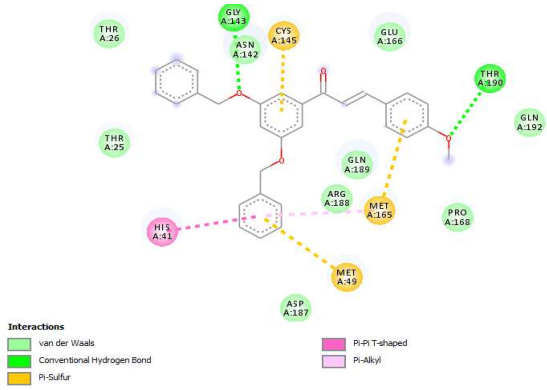

2D docking pose of **2**

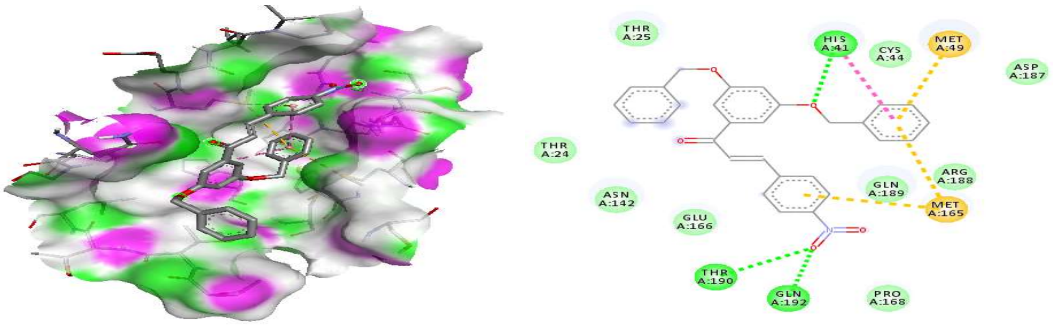

3D docking pose of **3** 2D docking pose of **3**

Figure-3 : Docking poses of compounds **1-3** with Sars-Cov-19 protease

3.4 ADMET evaluation

In this section, the pharmacokinetic parameters of compounds (**1-3**) were obtained and tabulated as in **Table-6** in accordance with the criteria defined above. These parameters were obtained with the help of Pre-ADME web page (http://www.swissadme.ch/) and molinspiron tool. According to the obtained results, the synthesized chalcone compounds (**1-3**) meets these criteria in other words as can be seen the theoretical ADME results of the synthesized are in agreement with the five rule of Lipinski.

All the molecules studied showed a number of hydrogen bond acceptors and hydrogen bond donors less than ten and five, respectively. Also, the number of rotatable bonds in each molecule was less than or equal to 10. Topological polar surface area (TPSA) is a very useful descriptor for prediction of transport of drug molecule across the biological barriers and was observed less than 130 $Å^2$ in the range of 80–96$Å^2$ (% ABS). The partition coefficient between n-octanol and water ($LogP_{o/w}$) is the classical descriptor for hydrophobicity. All the compounds (**1-3**) studied were found to have Log P values nearly 5.08 to 5.81 indicating moderate permeability across the cell membrane. These parameters exhibited that the studied compounds obeyed Lipinski's rule of five [42] with one violation and thus could be good orally active agents.

Table-6 : ADMET and Drug likeness properties of compounds **1-3**

Pre-ADMET	**Compounds**			**Drug likeness**	**Compounds**		
Property	**1**	**2**	**3**	**Property**	**1**	**2**	**3**
BBB C_{brain}/C_{blood}	0.67	0.35	0.41	CLogP	5.76	5.81	5.08
Invitro Caco-2 (nm/sec)	26.22	55.66	27.74	M.Wt	420.51	450.53	465.5
CYP2C19 inhibitor	Yes	Yes	Yes	HBA	3	4	5
CYP2D6 inhibitor	No	No	No	HBD	0	0	0
Volume	396.24	421.79	419.58	MDDR like Rule	Drug-like	Drug-like	Drug-like
TPSA	35.54	44.77	81.36	Lipinski violations	1	1	0

%ABS	96.74	93.55	80.93	Synthetic Accessibility	3.51	3.66	3.59
HIA(%)	99.03	98.14	97.65	WDI like Rule	90%	90%	90%
MDCK(nm/sec)	9.75	0.07	0.06	**Toxicity**	**Compounds**		
iPPB	100	100	100	**Property**	**1**	**2**	**3**
C LogP	5.76	5.81	5.08	hERG inhibition	medium risk	low risk	low risk
Log S	-6.58	-6.65	-6.64	Toxic Carcino Rat	negative	negative	negative
				PAINS/alerts	0	0	0

HBA hydrogen bond acceptor, ≤ 10; HBD hydrogen bond donor, ≤ 5; n-rotb no. of rotatable bonds, ≤ 10; TPSA topological polar surface area, ≤ 130 Å2; Log Po/w octanol/water partition coefficient, − 0.7 to + 5.0; Log S, aqueous solubility scale: Insoluble < − 10 < Poorly < − 6 < Moderately < − 4 < Soluble < − 2 < Very Soluble < 0 < Highly soluble; BBB blood-brain barrier permeability, central nervous system toxicity; CYP2D6 inhibitor hepatotoxicity; Lipinski number of violations of Lipinski's rule of five, maximum is 4; carcino test carcinogenicity, positive or negative; HIA human intestinal absorption.

The solubility of a molecule is a significant property influencing absorption. Also, a water-soluble compound facilitates the ease of formulation and oral administration to deliver a sufficient quantity of active ingredient [43]. The computational data revealed that none of the compounds crosses the blood-brain barrier and hence less possibility to produce neurotoxicity. CYP2D6 belongs to the superfamily of cytochrome P450 (CYP450) which is the most crucial isoenzyme that is responsible for metabolizing most of the drugs in the liver [44]. Inhibition of these enzymes causes drug–drug interaction leading to toxic effects due to accumulation and reduced elimination of drugs or its metabolites [43]. The results revealed that none of the compounds is inhibiting this essential enzyme.

Diabetic patients are at higher risk of developing cardiovascular disease as it is a common diabetes associated complication [45]. The inhibition of human ether-a-go-go-related gene (hERG) causes prolongation of QT interval leading to fatal ventricular tachyarrhythmia [46]. Compounds **2** and **3** were found to be at low-risk of hERG inhibition whereas **1** at moderate risk. Carcinogenicity is a toxicity that causes cancer in the body. The results specify that all the compounds (**1-3**) were non-carcinogenic thus stating the safety of compounds in the thriving drug development. Human intestinal absorption (HIA) data are the sum of bioavailability and absorption estimated from the ratio of excretion or cumulative excretion in urine, bile, and feces. The compounds are considered as well absorbed if the absorption is in the range of 70–100%. All the compounds evaluated were found to exhibit high intestinal absorption (HIA) in the range of 97.65 to 99.03 and excellent plasma protein binding (PPB) nature (100%). Then the MDR like rule of these compounds reveals that all has drug-like property.

Conclusion

In the present research, three substituted chalcones **1-3** have been synthesized by ultrasonic energy utilization method results better yields with low time. Componds 1-3 are characterized by UV, IR and NMR spectra. From these spectra, the position and nature functionalities, different carbons and protons are identified and confirmed their formation. The coupling constant values indicated the *trans* isomer of chalcones are formed. The DFT calculation of dihedral angles also supported these isomer conformations. DFT analyses of **1-3** are carried out and the bond parameters are calculated and agreed with literature. The compound **2** has shown good NLO property than others two compounds. The FMOs are calculated with their energies and showed that all the compounds possessed the charge transfer tendency. Further the molecular docking is performed and resulted that all the compounds have shown better binding with protease selected. The ADMET properties are noted and discussed. The compound 3 has obey all the Lipinkis rule and all are non-toxic. They showed drug like property.

Acknowledgement:

The author thank to the Department of Chemistry, Govt. Arts College, Chidambaram for providing research facilities for doing this work.

Reference:

[1] B. Sharma, S. C. Agrawal, and K. C. Gupta, "Colour reactions of chalcones and their mechanism (A review)," *Orient. J. Chem.*, vol. 24, no. 1, pp. 289–294, 2008.

[2] F. Atta-ur-Rahman, *Studies in Natural Products Chemistry*, First edit. 2013.

[3] N. P. Buu-Hoï and P. Cagniant, "A Novel Potential Anticancer Chalcone: Synthesis, Crystal Structure and Cytotoxic Assay," *Recl. des Trav. Chim. des Pays-Bas*, vol. 64, no. 8, pp. 214–218, 1945.

[4] N. Y. S. Jayapal .Maleraju, "Synthesis of chalcones by a claisen – schmidt reaction using magnesium hydrogen sulphate as a catalyst under solvent – free condition," vol. 3, no. 1, pp. 37–40, 2013.

[5] S. Mandge, H. Singh, and S. Gupta, "Synthesis and characterization of some chalcone derivatives," *Trends Appl. Sci. Res.*, vol. 2, no. 1, pp. 52–56, 2007.

[6] V. I. Hugo, "Synthesis and antimicrobial screening of some quinonoid systems," vol. 7, no. 1, pp. 40–45, 1996.

[7] Z. J. Cheng, S. C. Kuo, S. C. Chan, F. N. Ko, and C. M. Teng, "Antioxidant properties of butein isolated from Dalbergia odorifera," *Biochim. Biophys. Acta - Lipids Lipid Metab.*, vol. 1392, no. 2–3, pp. 291–299, 1998.

[8] A. P. S. Bonakdar, F. Vafaei, M. Farokhpour, M. H. N. Esfahani, and A. R. Massah, "Synthesis and anticancer activity assay of novel chalcone-sulfonamide derivatives," *Iran. J. Pharm. Res.*, vol. 16, no. 2, pp. 565–568, 2017.

[9] T. Moreira Osório *et al.*, "Antibacterial activity of chalcones, hydrazones and oxadiazoles against methicillin-resistant Staphylococcus aureus," *Bioorganic Med. Chem. Lett.*, vol. 22, no. 1, pp. 225–230, 2012.

[10] V. Kuete and L. P. Sandjo, "Isobavachalcone: An overview," *Chin. J. Integr. Med.*, vol. 18, no. 7, pp. 543–547, 2012.

[11] A. Gómez-Rivera, H. Aguilar-Mariscal, N. Romero-Ceronio, L. F. Roa-De La Fuente, and C. E. Lobato-García, "Synthesis and anti-inflammatory activity of three nitro chalcones," *Bioorganic Med. Chem. Lett.*, vol. 23, no. 20, pp. 5519–5522, 2013.

[12] Y. J. Wang *et al.*, "Synthesis and antiviral bioactivity of novel chalcone derivatives containing purine moiety," *Chinese Chem. Lett.*, vol. 29, no. 1, pp. 127–130, 2018.

[13] B. B. Chavan, A. S. Gadekar, P. P. Mehta, P. K. Vawhal, A. K. Kolsure, and A. R. Chabukswar, "Synthesis and Medicinal Significance of Chalcones-A Review," *Asian J. Biomed. Pharm. Sci.*, vol. 6, no. 56, pp. 01–07, 2015.

[14] M. Larsen, H. Kromann, A. Kharazmi, S.F. Nielsen, Conformationally restricted anti-plasmodial chalconesBioorg, Med. Chem. Lett 15 (2005) 4 858–4 861, doi: 10.1016/j.bmcl.2005.07.012 .

[15] Kumar, A.; Kumar, R.; Gupta, A.; Tandon, P.; D'silva, E.D. Molecular Structure, Nonlinear Optical Studies and Spectroscopic Analysis of Chalcone Derivative (2E)-3-[4-(Methylsulfanyl) Phenyl]-1-(3-Bromophenyl) Prop-2-En-1-One by DFT Calculations. J. Mol. Struct. 2017, 1150, 166–178.

[16] Alwani Zainuri, D.; Arshad, S.; Che Khalib, N.; Fikri Zaini, M.; Razak, I.A. Molecular Structure Investigation On Organic Chalcone Derivative of (E)-3-(4-Bromothiophen-2-1-(3-Nitrophenyl)Prop-2-En-1-One: A Combined Experimental and Theoretical Study. J. Phys. Conf. Ser. 2018, 1083, 12046.

[17] Zaini, M.F.; Arshad, S.; Thanigaimani, K.; Khalib, N.C.; Zainuri, D.A.; Abdullah, M.; Razak, I.A. New Halogenated Chalcones: Synthesis, Crystal Structure, Spectroscopic and Theoretical Analyses for Third-Order Nonlinear Optical Properties. J. Mol. Struct. 2019, 1195, 606–619.

[18] Chidan Kumar, C.S.; Govindarasu, K.; Fun, H.-K.; Kavitha, E.; Chandraju, S.; Quah, C.K. Synthesis, Molecular Structure, Spectroscopic Characterization and Quantum Chemical Calculation Studies of (2E)-1-(5-Chlorothiophen-2-Yl)-3-(2,3,4-Trimethoxyphenyl)Prop-2-En-1-One. J. Mol. Struct. 2015, 1085, 63–77.

[19] Yalcin, G.; Burmaoglu, S.; Yildiz, I.; Algul, O. Molecular Docking Studies on Fluoro-Substituted Chalcones as Potential DprE1 Enzyme Inhibitors. J. Mol. Struct. 2018, 1164, 50–56.

[20] Hussein, R.K.; Elkhair, H.M. Molecular Docking Identification for the Efficacy of Some Zinc Complexes with Chloroquine and Hydroxychloroquine against Main Protease of COVID-19. J. Mol. Struct. 2021, 1231, 129979.

[21] Nayak, P.S.; Narayana, B.; Sarojini, B.K.; Fernades, J.; Bharath, B.R.; Madhu, L.N. Synthesis, Molecular Docking and Biological Evaluation of Novel Bis-Pyrazole Derivatives for Analgesic, Anti-Inflammatory and Antimicrobial Activities. Med. Chem. Res. 2015, 24, 4191–4206.

[22] Khan, S. A., Zia, K., Ashraf, S., Uddin, R., & Ul-Haq, Z. (2020). Identification of chymotrypsin-like protease inhibitors of SARS-CoV-2 via integrated computational approach. *Journal of Biomolecular Structure and Dynamics*, *0*(0), 1–10. https://doi.org/10.1080/07391102.2020.1751298

[23] Park, J. Y., Ko, J. A., Kim, D. W., Kim, Y. M., Kwon, H. J., Jeong, H. J., Ryu, Y. B. (2016a). Chalcones isolated from Angelica keiskei inhibit cysteine proteases of SARS-

CoV. *Journal of Enzyme Inhibition and Medicinal Chemistry*, *31*(1), 23–30. https://doi.org/10.3109/14756366.2014.1003215

[24] Park, J. Y., Yuk, H. J., Ryu, H. W., Lim, S. H., Kim, K. S., Park, K. H., Lee, W. S. (2017). Evaluation of polyphenols from Broussonetia papyrifera as coronavirus protease inhibitors. *Journal of Enzyme Inhibition and Medicinal Chemistry*, *32*(1), 504–512. https://doi.org/10.1080/ 14756366.2016.1265519

[25] Vijayakumar, B. G., Ramesh, D., Joji, A., Jayachandra, J., & Kannan, T. (2020). In silico pharmacokinetic and molecular docking studies of natural flavonoids and synthetic indole chalcones against essential proteins of SARS-CoV-2. *European Journal of Pharmacology*, *886*, 173448.

[26] Alsafi, M. A., Hughes, D. L., & Said, M. A. (2020). First COVID-19 molecular docking with a chalcone-based compound: Synthesis, single crystal structure and Hirshfeld surface analysis study. *Acta Crystallographica Section C:Structural Chemistry*, *76*, 1043–1050. https://doi.org/10.1107/S2053229620014217

[27] R. Guptha, N. Guptha and A. Jain, Improved synthesis of chalcones and pyrazolines under ultrasonic irradiation, Ind. J. Chem. 49B (2010) 351-355.

[28] Frisch, M.J.; Trucks, G.W.; Schlegel, H.B. Gaussian 09; Gaussian Inc.: Wallingford, CT, USA, 2009

[29] M. Prabuswamy, S.M. Kumar, D. Bhuvaneshwar, Ch.S.S.S. Murthy, N.K. Lokanatha, 1-(2-Fluorophenyl)-3-(2,4,6-trimethoxyphenyl)prop-2-en-1-one, Acta Cryst. E 68 (2012) o3190.

[30] Galabov, B.; Simov, D. The Stretching Vibration of Carbonyl Groups in Cyclic Ketones. Chem. Phys. Lett. **1970**, 5, 549–551.

[31] Ahmed M. Deghady, Rageh K. Hussein, Abdulrahman G. Alhamzani and Abeer Mera, Density Functional Theory and Molecular Docking Investigations of the Chemical and Antibacterial Activities for 1-(4-Hydroxyphenyl)-3-phenylprop-2-en-1-one, Molecules 2021, 26, 3631. https://doi.org/10.3390/molecules26123631

[32] Balan, V.; Mihai, C.-T.; Cojocaru, F.-D.; Uritu, C.-M.; Dodi, G.; Botezat, D.; Gardikiotis, I. Vibrational Spectroscopy Fingerprinting in Medicine: From Molecular to Clinical Practice. Materials **2019**, 12, 2884.

[33] Gipson, K.; Stevens, K.; Brown, P.; Ballato, J. Infrared Spectroscopic Characterization of Photoluminescent Polymer Nanocomposites. J. Spectrosc. **2015**, 2015, 1–9.

[34] Adhikari, S. &Kar, T. (2012). Experimental and theoretical studies on physicochemical properties of L-leucine nitrate- a probable nonlinear optical material. *J. Crys. Growth.* 356: 4-9. DOI: 10.1016/j.jcrysgro.2012.07.008

[35] A. N. Castro, F. A. P. Osório, R. R. Ternavisk, H. B. Napolitano, C. Valverde, and B. Baseia, "Theoretical investigations of nonlinear optical properties of two crystalline acetamides structures including polarization effects of their environment", *Chem. Phys. Lett.*, vol. 681, pp. 110–123, 2017. DOI: https://doi.org/10.1016/j.cplett.2017.05.066.

[36] N.R. Sheela, S. Muthu, S. Sampathkrishnan, Molecular orbital studies (hardness, chemical potential and electrophilicity), vibrational investigation and theoretical NBO analysis of 4-4'-(1H-1,2,4-triazol-1-yl methylene) dibenzonitrile based on abinitio and

DFT methods., Spectrochim. Acta Part A 120 (2014) 237–251, doi: 10.1016/j.saa.2013.10.007 .

[37] Berman, H. M., Henrick, K., Nakamura, H. (2003). Announcing the worldwide Protein Data Bank, Nature Structural Biology,10(12), 980.

[38] Trott, O., & Olson, A. J. (2010). AutoDock Vina: Improving the speed and accuracy of docking with a new scoring function, efficient optimization, and multithreading. Journal of Computational Chemistry, 31(2), 455–461. https://doi.org/10.1002/jcc.21334

[39] de Lima, W. E. A., Francisco, A., da Cunha, E. F., Radic, Z., Taylor, P., Franc¸a, T. C., & Ramalho, T. C. (2017). Mechanistic studies of new oximes reactivators of human butyryl cholinesterase inhibited by cyclosarin and sarin. Journal of Biomolecular Structure & Dynamics, 35(6), 1272–1282. https://doi.org/10.1080/07391102.2016.1178173

[40] Ea de Lima, W., F Pereira, A., A de Castro, A., Ff da Cunha, E., & C Ramalho, T. (2016). Flexibility in the molecular design of acetylcholinesterase reactivators: Probing representative conformations by chemometric techniques and docking/QM calculations. Letters in Drug Design & Discovery, 13, 360–371.

[41] Kuca, K., Musilek, K., Jun, D., Zdarova-Karasova, J., Nepovimova, E.,Soukup, O., Hrabinova, M., Mikler, J., Franca, T. C. C., Da Cunha,E. F. F., De Castro, A. A., Valis, M., & Ramalho, T. C. (2018). A newly developed oxime K203 is the most effective reactivator of tabuninhibited acetylcholinesterase. BMC Pharmacology and Toxicology, 19(1), 1–10. https://doi.org/10.1186/s40360-018-0196-3

[42] Lipinski CA (2004) Lead- and drug-like compounds: The rule-of-five revolution. Drug Discov Today Technol 1:337–341. https://doi.org/10.1016/j.ddtec.2004.11.007

[43] Daina A, Michielin O, Zoete V (2017) SwissADME: a free web tool to evaluate pharmacokinetics, drug-likeness and medicinal chemistry friendliness of small molecules. Sci Rep 7:42717. https://doi.org/10.1038/srep42717

[44] Rydberg P, Olsen L (2012) Predicting drug metabolism by cytochrome P450 2C9: comparison with the 2D6 and 3A4 Isoforms. ChemMedChem 7:1202–1209. https://doi.org/10.1002/cmdc.201200160

[45] Aldossari KK (2018) Cardiovascular outcomes and safety with antidiabetic drugs. Int J Health Sci (Qassim) 12:70–83

[46] Guth BD, Rast G (2010) Dealing with hERG liabilities early: diverse approaches to an important goal in drug development. Br J Pharmacol 159:22–24. https://doi.org/10.1111/j.1476-5381.2009.00265.x